Supplemental File 2: TotBlocks assembly guide

Table of Contents

S2.1 Introduction 2

S2.2 2:1 phyllosilicates (mica group) 2

S2.3 Pyribole series 3

S2.3.1 Pyroxene group 3

S2.3.2 Amphibole supergroup 6

S2.3.3 Clinojimthompsonite 7

S2.3.4 Chesterite 8

S2.4 Palysepiole series 9

S2.4.1 Palygorskite group 9

S2.4.2 Sepiolite group 10

S2.4.3 Kalifersite 11

S2.5 Other layered minerals 12

S2.5.1 Brucite group and gibbsite 12

S2.5.2 Kaolinite-serpentine group 13

S2.5.3 Chlorite group 14

S2.6 Supplemental videos 14

S2.7 References 15

S2.1 Introduction

In this guide, we will walk you through how to construct different crystal structures using TotBlocks (video abstract: https://doi.org/10.5446/57470). Supplemental Video 2 (https://doi.org/10.5446/57471) contains an overview of each of the component pieces of TotBlocks, demonstrates how to assemble modules, and illustrates the different linkages between modules. All of the component pieces of TotBlocks and the source code used to produce them can be found on the Github repository (Leung, 2020; https://doi.org/10.5281/zenodo.5240816). Supplemental Video 13 (https://doi.org/10.5446/57483) describes the process of 3D printing TotBlocks.

S2.2 2:1 phyllosilicates (mica group)

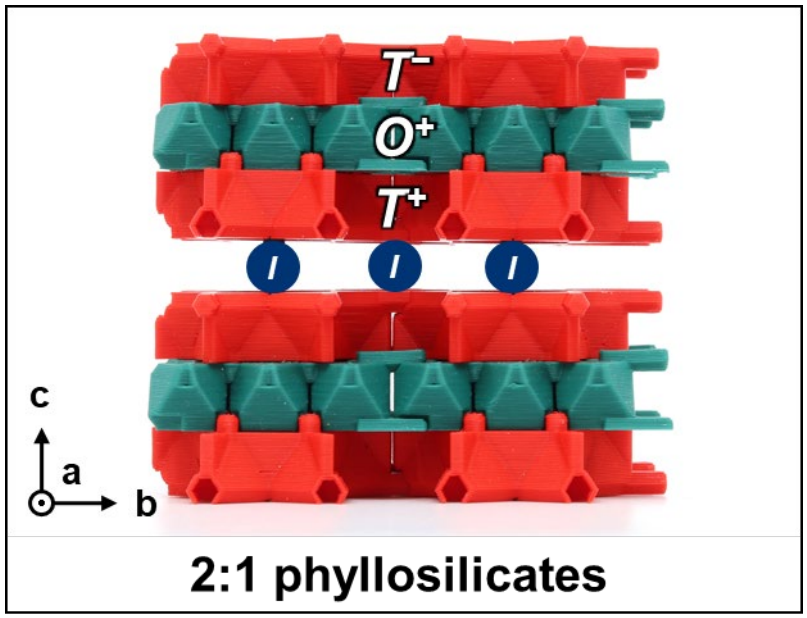

Fig. S2.1 The crystal structure of the 2:1 phyllosilicates (mica group).

Mica-group minerals are the most important rock-forming minerals of the 2:1 phyllosilicates. To build the mica structure as shown in Fig. S2.1, connect two sets of two double-chain-width *T-O-T* modules (see Fig. S1.2c–d) such that there is no vertical offset between the modules (phyllosilicate-type linkage; Fig. 2b). There will be sites missing between the linked double-chain modules where single octahedron pieces can be added (Fig. S1.3a). The adjoined *T-O-T* modules represent the sheeted structure of the 2:1 phyllosilicates. To vertically stack individual sheets, vertical pegs (Fig. S1.3b) are inserted into the slots of the *O* layer to form the connection.

Supplemental Video 3 (https://doi.org/10.5446/57472) demonstrates the construction of this mineral structure.

S2.3 Pyribole series

S2.3.1 Pyroxene group

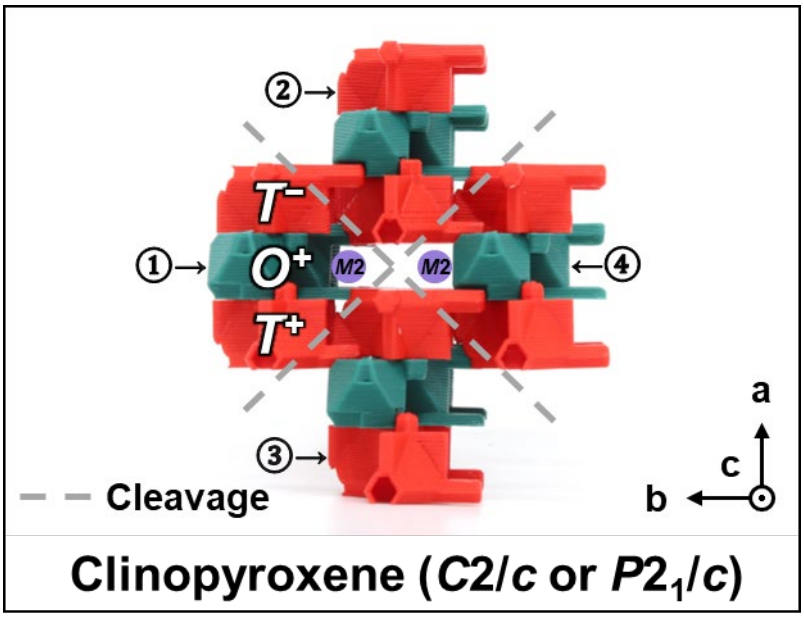

Fig. S2.2 The crystal structure of clinopyroxene.

The simplest pyroxene structure, clinopyroxene (Fig. S2.2), consists of *T*-*O*-*T* rod modules that only use O^+ modules, producing the vertical stacking sequence ++++ (Thompson, 1981). This results in a stacking offset along the length of the rod modules that leads to monoclinic symmetry (see Sect. 5.1.3 for a discussion on polytypes and symmetry). To construct the clinopyroxene structure using TotBlocks, connect one single-chain-width T-O^+-T module (see Fig. S1.2a–b; labelled as ① in Fig. S2.2) to a second single-chain-width module ② such that the T^- module of the first ① is joined to the bottom of the O^+ module of the second ② (and top of O^+ of ① joined to T^+ of ②). A third single-chain-module ③ can then be joined so that the T^+ of the first module ① is joined to the top of the O^+ module of the third (and bottom of O^+ of ① joined to the T^- of ②). This pattern can then be repeated as needed to extend the structure. In Fig. S2.2, a fourth T-O^+-T module ④ is joined to the second ② and third ③ T-O^+-T modules.

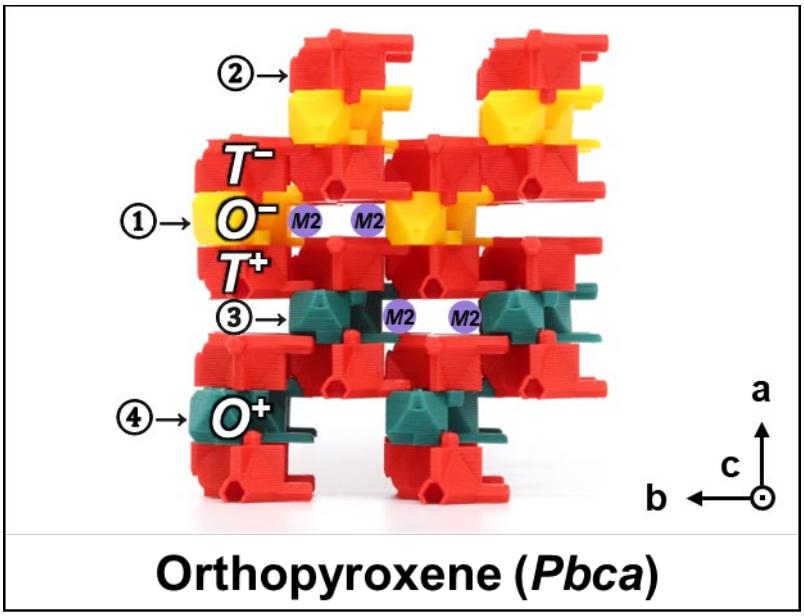

Fig. S2.3 The crystal structure of orthopyroxene.

Other pyroxene polytypes incorporate more variation with respect to the orientation of the *O* modules. The orthopyroxene structure (Fig. S2.3) consists of corrugated rows of *T*-*O*-*T* rod modules that contain O^+ modules, alternating with corrugated rows containing O^- modules. This yields the vertical stacking pattern ++−− (Thompson, 1981). To construct the orthopyroxene structure, four single-chain-width *T*-*O*-*T* modules must be made (see Fig. S1.2a–b). Two of these modules will use O^+ and two will use O^-. Using a *T*-O^--*T* module ①, connect the T^- to the bottom of the O^- of another *T*-O^--*T* module ② (the top of O^- for ① will also join to T^+ of ②). Then, connect the T^+ of ① to the top of the O^+ of a *T*-O^+-*T* module ③ (the bottom of O^- for ① will also join to T^- of ③). The final *T*-O^+-*T* module ④ will be connected to the structure by linking its T^- to the base of the O^+ of three connected single-chain-width modules (the top of the O^+ of ④ will also be joined to T^+ of ③). This pattern can then be repeated (starting again with *T*-O^--*T*) to extend the structure. In Fig. S2.3, two iterations of these instructions are shown.

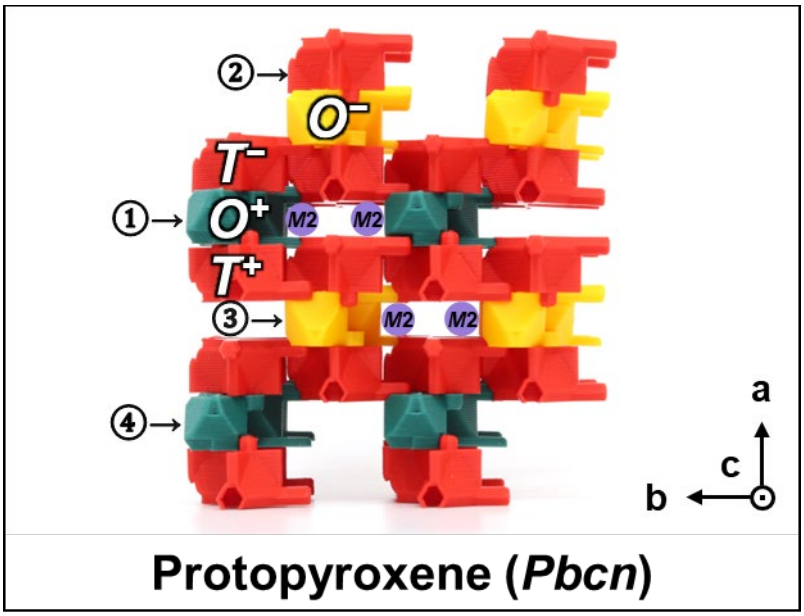

Fig. S2.4 The crystal structure of protopyroxene.

Conversely, the protopyroxene structure (Fig. S2.4) consists of rows of *T*-*O*-*T* modules with alternating O^+ and O^- modules, yielding the vertical stacking pattern +–+– (Thompson, 1981). As in orthopyroxene, the protopyroxene structure can be constructed with four single-chain-width *T*-*O*-*T* modules (two O^+ and two O^-). However, the O^+ modules are always linked to O^- modules and vice versa. Specifically, using a *T*-O^+-*T* module ① (Fig. S1.2a–b), connect the T^- to the bottom of the O^- of a *T*-O^--*T* module ② (top of O^+ of ① will also connect to T^+ of ②) and the T^+ to the top of the O^- of the second *T*-O^--*T* module ③ (bottom of O^+ of ① will also connect to T^- of ③). The final *T*-O^+-*T* module ④ will be connected to the structure by linking its T^- to the base of the O^- of three connected single-chain-width modules (top of O^+ of ④ will also link to T^+ of ③). This pattern can then be repeated (starting again with *T*-O^+-*T*) to extend the structure. In Fig. S2.4, two iterations of these instructions are shown.

Supplemental Video 4 (https://doi.org/10.5446/57473) demonstrates the construction of the three pyroxene polytypes.

S2.3.2 Amphibole supergroup

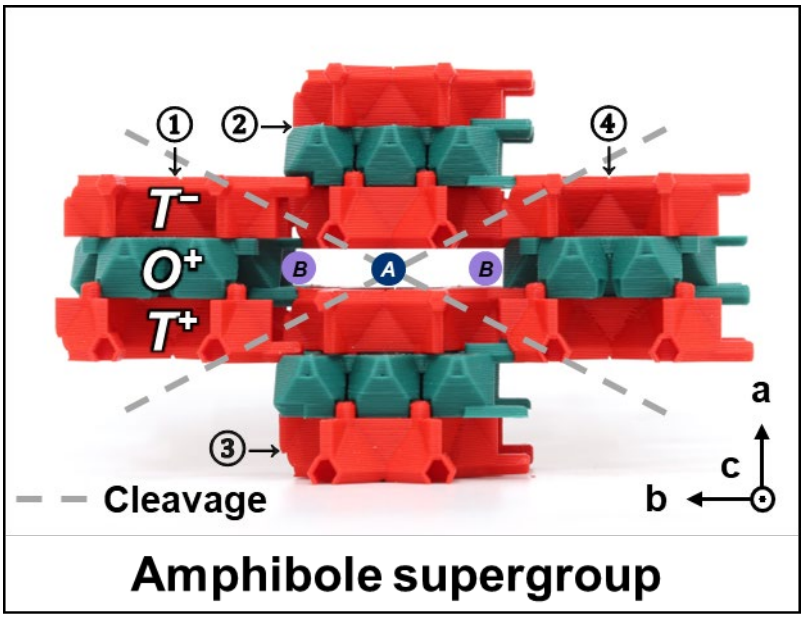

Fig. S2.5 The crystal structure of the amphibole supergroup.

To construct the amphibole structure as shown in Fig. S2.5, connect one double-chain-width T-O^+-T module (see Fig. S1.2c–d; labelled as ① in Fig. S2.5) to a second double-chain-width module ②, such that the T^- module of ① is joined to the bottom of the O^+ module of ② (the top of O^+ for ① will also connect to the T^+ of ②). A third double-chain module ③ can then be joined so that the T^+ of the first module ① is joined to the top of the O^+ module of the third ③ (the bottom of O^+ for ① should also join to the T^- of ③). This pattern can then be repeated as needed to extend the structure. In Fig. S2.5, the structure is completed by joining a fourth module ④ to the second ② and third ③ modules.

Supplemental Video 5 (https://doi.org/10.5446/57474) demonstrates the construction of this mineral structure.

S2.3.3 Clinojimthompsonite

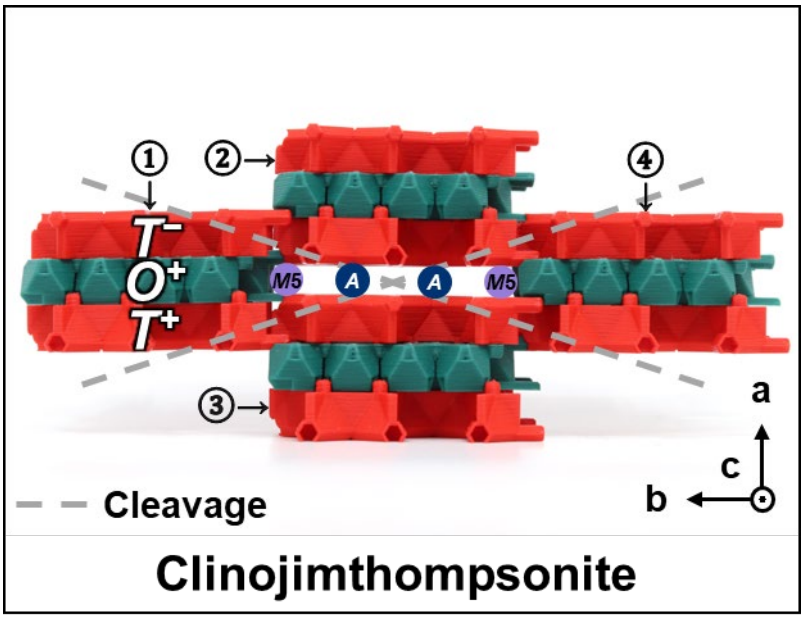

Fig. S2.6 The crystal structure of clinojimthompsonite.

To construct the clinojimthompsonite structure as shown in Fig. S2.6, connect one triple-chain-width *T*-*O*-*T* module (see Fig. S1.2e–f; labelled as ① in Fig. S2.6) to a second triple-chain-width module ② such that the T^- module of the first is joined to the bottom of the O^+ module of the second (the top of the O^+ module in ① will also be joined to the T^+ of ②). A third triple-chain-module ③ can then be joined so that the T^+ of the first module ① is joined to the top of the O^+ module of ③ (the bottom of the O^+ of ① is concurrently joined to the T^- of ③). This pattern can then be repeated as needed to extend the structure. In Fig. S2.6, a fourth module ④ is joined to the second ② and third ③ modules.

Supplemental Video 6 (https://doi.org/10.5446/57475) demonstrates the construction of this mineral structure and that of chesterite.

S2.3.4 Chesterite

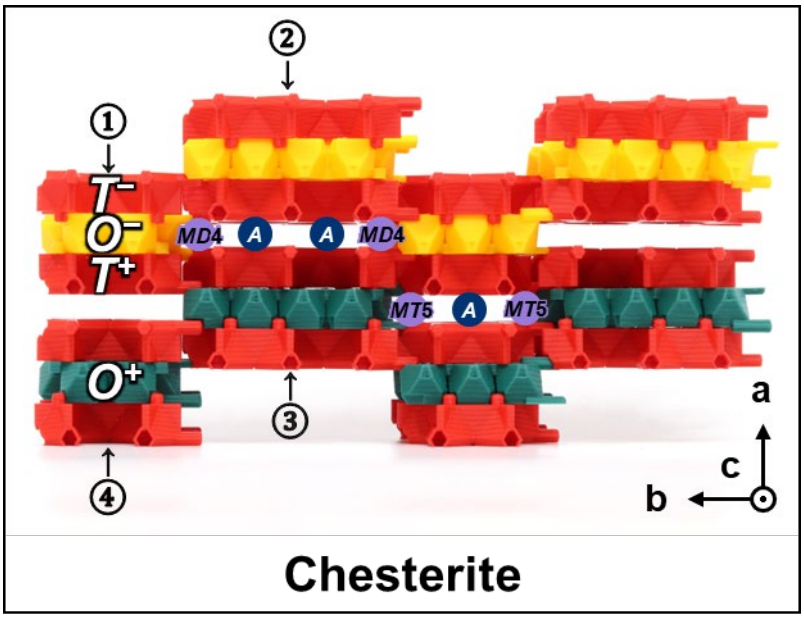

Fig. S2.7 The crystal structure of chesterite.

To construct the chesterite structure as shown in Fig. S2.7, two double-chain-width *T*-*O*-*T* modules (one O^+ and one O^-; Fig. S1.2c–d) and two triple-chain-width *T*-*O*-*T* modules (one O^+ and one O^-; Fig. S1.2e–f) are needed. The T^- of the double-chain-width T-O^--T module (labelled as ① in Fig. S2.7) is connected to the base of the O^- of the triple-chain-width T-O^--T module ② (the top of O^- in ① will concurrently be joined to the T^+ of ②). The T^+ of the first double-chain-width module ① is then connected to the top of the O^+ of the triple-chain-width T-O^+-T module ③ (the bottom of the O^- in ① will also be joined to the T^- of ③). The T^- of the final double-chain module (T-O^+-T) ④ is then connected to the base of the O^+ of the triple-chain-width module ③ (the top of the O^+ of ④ will be joined to the T^+ of ③). This pattern can then be repeated to extend the structure. In summary, the *T*-*O*-*T* modules are connected widthwise such that the T^- modules join to the bottom of the *O* modules and vice-versa (T^+ modules join to the top of the *O* modules), with the pattern alternating between double-chain-width and triple-chain-width modules. Additionally, after each double-chain-width and triple-chain-width pair, the included *O* modules alternate between using O^+ and O^-. This pattern results in alternating corrugated layers becoming visible in the crystal structure. Figure S2.7 shows two iterations of these instructions.

Supplemental Video 6 (https://doi.org/10.5446/57475) demonstrates the construction of this mineral structure and that of clinojimthompsonite.

S2.4 Palysepiole series

S2.4.1 Palygorskite group

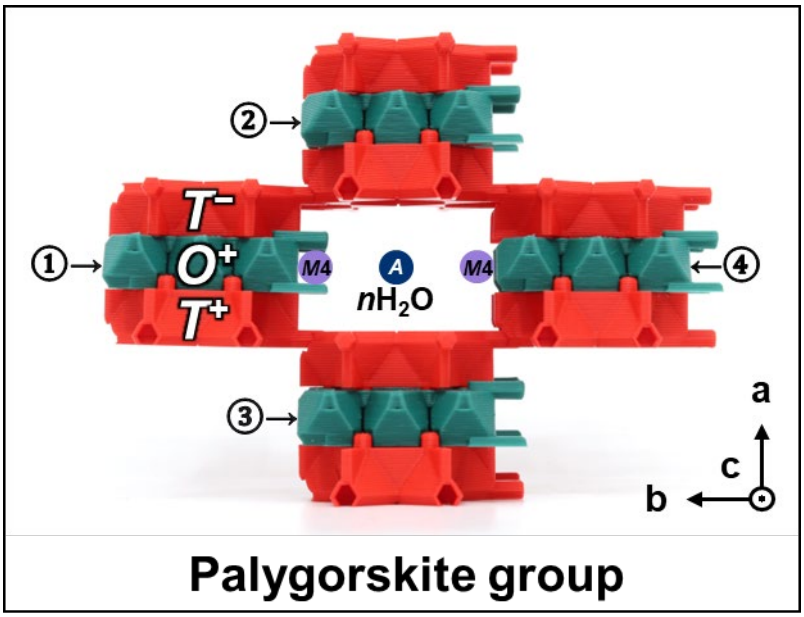

Fig. S2.8 The crystal structure of the palygorskite group.

To construct the palygorskite structure as shown in Fig. S2.8, connect one double-chain-width T-O^+-T module (S1.2c–d; labelled as ① in Fig. S2.8) to a second double-chain-width module ② such that the T^- module of the first ① is joined to the T^+ module of the second ②. A third double-chain-width module ③ can then be joined so that the T^+ of ① is joined to the T^- module of ③. This pattern can then be repeated as needed to extend the structure. Here, a fourth T-O^+-T module ④ is added to the second and third T-O^+-T modules, to close the gap and highlight the channel space.

Supplemental Video 7 (https://doi.org/10.5446/57476) demonstrates the construction of this mineral structure.

S2.4.2 Sepiolite group

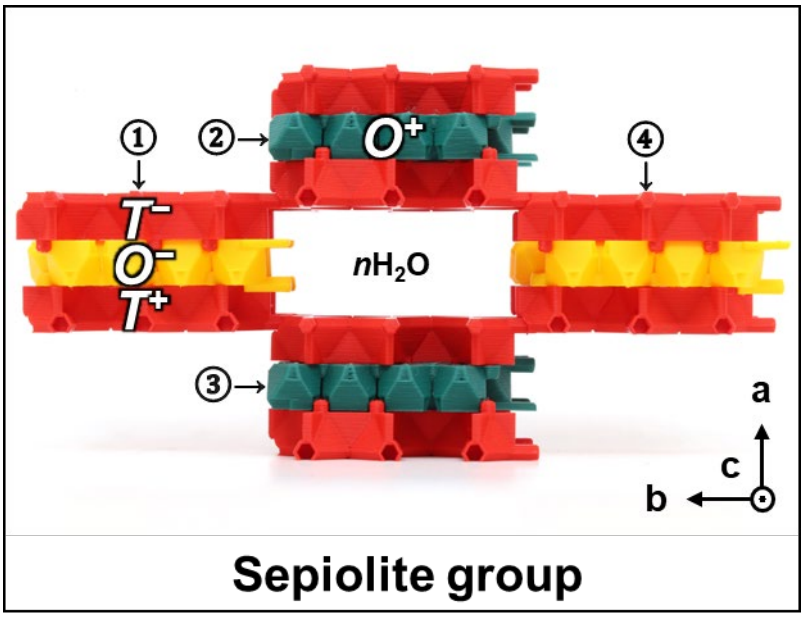

Fig. S2.9 The crystal structure of the sepiolite group.

To construct the sepiolite structure as shown in Fig. S2.9, one begins with three triple-chain-width *T*-*O*-*T* modules (two O^+ and one O^-; Fig. S1.2e–f). Specifically, using the T-O^--T module (labelled as ① in Fig. S2.9), connect the T^- to the T^+ of a T-O^+-T module ②. The T^+ of the T-O^--T module ① is then connected to the T^- of second T-O^+-T module ③. The pattern can then be repeated to extend the structure. In Fig. S2.9, a fourth (T-O^--T) module ④ is joined to the T-O^+-T modules, to close the gap and highlight the channel space. As seen in the construction of the protopyroxene structure, the O^+ modules always link to O^- modules and vice versa, resulting in an alternating pattern.

Supplemental Video 8 (https://doi.org/10.5446/57477) demonstrates the construction of this mineral structure.

S2.4.3 Kalifersite

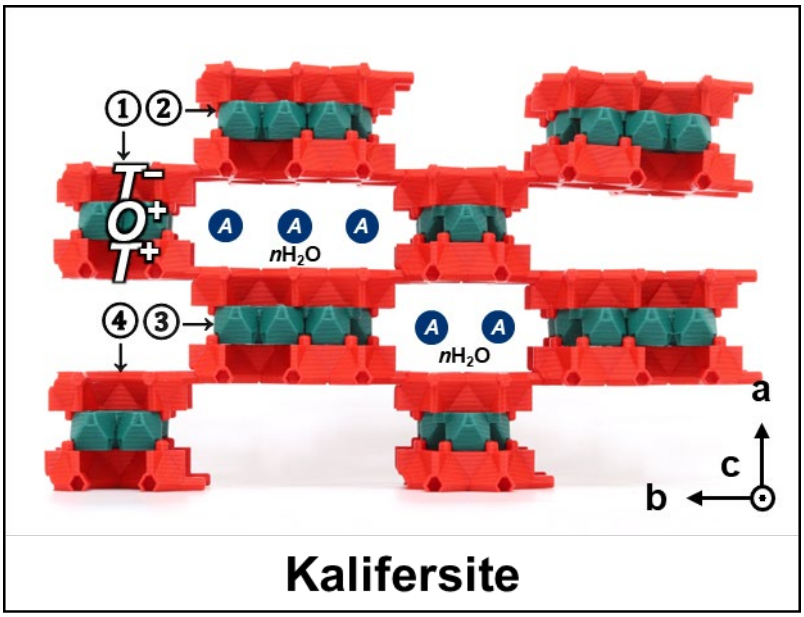

Fig. S2.10 The crystal structure of kalifersite.

When building the crystal structure of kalifersite, the same *T* modules (Fig. S1.2d and f) used in other crystal structures will be used, but mineral-specific O^+ modules (Z_3 and Z_6) must be printed (see README file in Leung (2022); https://doi.org/10.5281/zenodo.5240816).

To construct the kalifersite structure as shown in Fig. S2.10, two double-chain-width T-O^+-T modules (constructed using Z_3 O^+ modules; Fig. S1.4) and triple-chain-width T-O^+-T modules (constructed using Z_6 O^+ modules; Fig. S1.4) are needed. The T^- module of one double-chain-width module (labelled as ① in Fig. S2.10) is connected to the T^+ of a triple-chain-width module ②. The T^+ module of the double-chain-width module ① is then connected to the T^- module of the second triple-chain-width module ③. The T^+ of this second triple-chain-module ③ is then connected to the T^- module of a second double-chain-width module ④. This pattern can then be repeated as needed to extend the structure. Figure S2.10 shows two iterations of these instructions.

Supplemental Video 9 (https://doi.org/10.5446/57479) demonstrates the construction of this mineral structure.

S2.5 Other layered minerals

S2.5.1 Brucite group and gibbsite

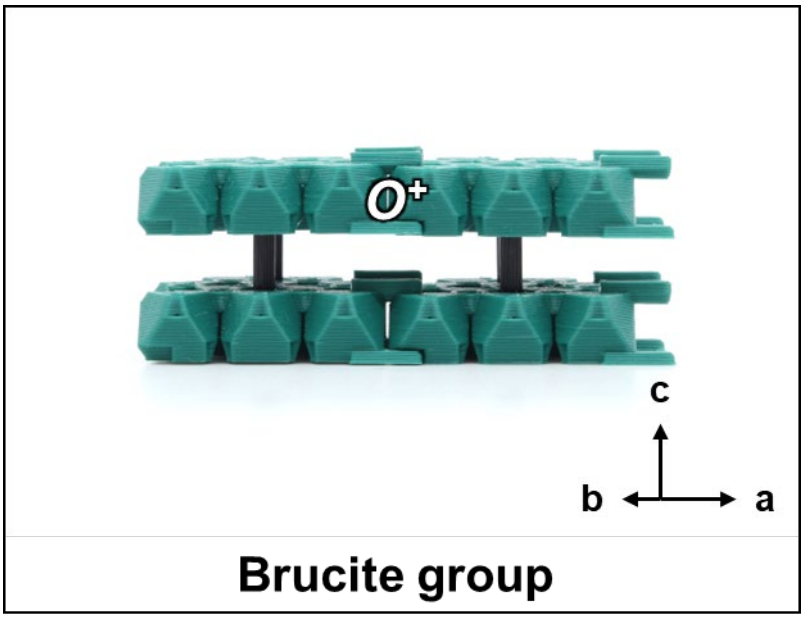

Fig. S2.11 The crystal structure of the brucite group.

To construct the brucite structure as shown in Fig. S2.11, connect double-chain-width O^+ modules (Fig. S1.2d) widthwise to illustrate the sheeted nature of the structure. Missing sites between the horizontally connected modules can be filled using single octahedron pieces (Fig. S1.3a). To vertically stack the sheets, pegs (Fig. S1.3b) are inserted into the slots of the *O* layer, with the triangular end being inserted into the bottom sheet.

Supplemental Video 10 (https://doi.org/10.5446/57480) demonstrates the construction of this mineral structure.

S2.5.2 Kaolinite-serpentine group

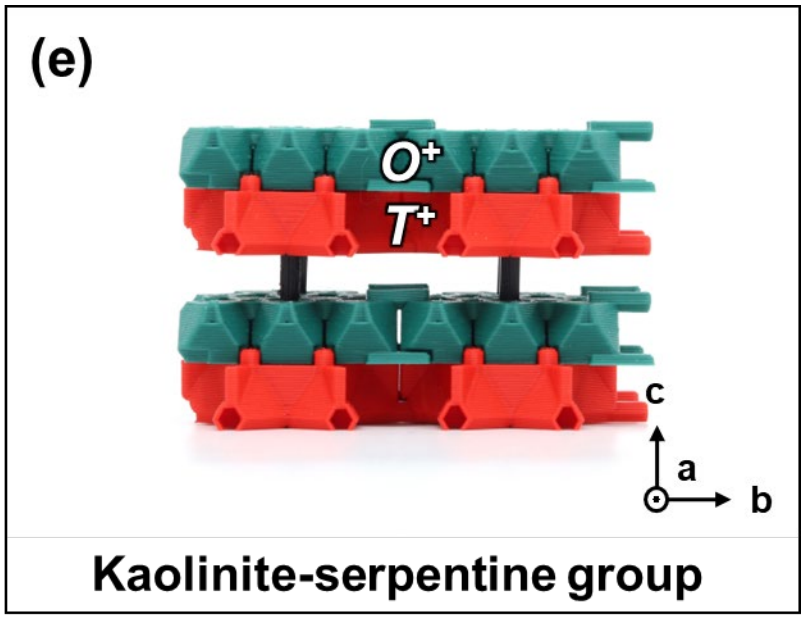

Fig. S2.12 The crystal structure of the kaolinite-serpentine group.

To construct the lizardite structure as shown in Fig. S2.12, vertically join double-chain-width T^+ modules to O^+ modules (Fig. S1.2d), forming *T*-*O* modules. These *T*-*O* modules can be joined widthwise such that there is no vertical offset between the connected modules, which illustrates the sheeted nature of the structure. Missing sites in the *O* layer can be filled using single octahedron pieces (Fig. S1.3a). To vertically stack the sheets, pegs (Fig. S1.3b) are inserted into the slots of the *O* layers, with the triangular end being inserted into the bottom sheet.

Supplemental Video 11 (https://doi.org/10.5446/57481) demonstrates the construction of this mineral structure.

S2.5.3 Chlorite group

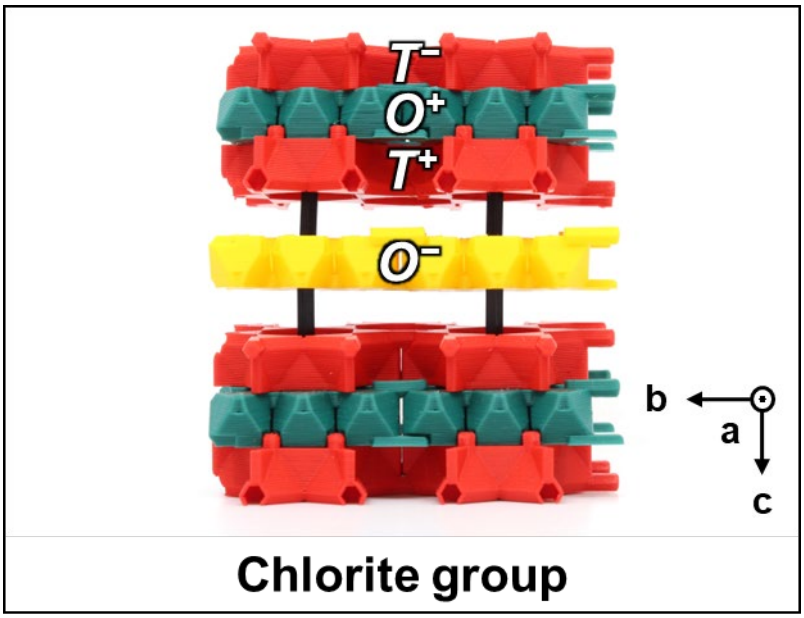

Fig. S2.13 The crystal structure of the chlorite group.

To construct the chlorite structure as shown in Fig. S2.13, assemble two sets of two double-chain-width T-O^+-T modules (Fig. S1.2c–d) and join these widthwise so that there is no horizontal offset. These represent the sheeted nature of the chlorite structure. There will be sites missing in the O layers between the T-O^+-T modules that can be filled using single octahedron pieces (Fig. S1.3a). Next, join two double-chain-width O^- modules (Fig. S1.2d) widthwise, with missing sites being filled by single octahedron pieces (Fig. S1.3a). Finally, vertically stack the T-O^+-T layers, with the O^- layer sandwiched between the two T-O^+-T layers, using vertical pegs that are inserted into the slots of the O layers (Fig. S1.3b). The triangular end of the vertical pegs will be inserted into the O^- modules.

Supplemental Video 12 (https://doi.org/10.5446/57482) demonstrates the construction of this mineral structure.

S2.6 Supplemental videos

The titles of Supplemental Videos 1–13 are listed as follows:

(1) TotBlocks Video Abstract (https://doi.org/10.5446/57470; Leung and dePolo, 2022a),
(2) Assembly of TotBlocks (https://doi.org/10.5446/57471; Leung and dePolo, 2022b),
(3) 2:1 Phyllosilicates (https://doi.org/10.5446/57472; Leung and dePolo, 2022c),
(4) Pyroxene Group (https://doi.org/10.5446/57473; Leung and dePolo, 2022d),

(5) Amphibole Supergroup (https://doi.org/10.5446/57474; Leung and dePolo, 2022e),
(6) Clinojimthompsonite and Chesterite (https://doi.org/10.5446/57475; Leung and dePolo, 2022f),
(7) Palygorskite Group (https://doi.org/10.5446/57476; Leung and dePolo, 2022g),
(8) Sepiolite Group (https://doi.org/10.5446/57477; Leung and dePolo, 2022h),
(9) Kalifersite (https://doi.org/10.5446/57479; Leung and dePolo, 2022i),
(10) Brucite Group (https://doi.org/10.5446/57480; Leung and dePolo, 2022j),
(11) Kaolinite-Serpentine Group (https://doi.org/10.5446/57481; Leung and dePolo, 2022k),
(12) Chlorite Group (https://doi.org/10.5446/57482; Leung and dePolo, 2022l),
(13) How to 3D Print TotBlocks (https://doi.org/10.5446/57483; Leung and dePolo, 2022m).

S2.7 References

Leung, D. D. V.: derekdvleung/totblocks: Totblocks 2022.05 (totblocks-2022.05), Zenodo [code], https://doi.org/10.5281/zenodo.5240816, 2022.

Leung, D. D. V. and dePolo, P. E.: TotBlocks Video Abstract, TIB-AV Portal [video], https://doi.org/10.5446/57470, 2022a.

Leung, D. D. V. and dePolo, P. E.: Assembly of TotBlocks, TIB-AV Portal [video], https://doi.org/10.5446/57471, 2022b.

Leung, D. D. V. and dePolo, P. E.: 2:1 Phyllosilicates, TIB-AV Portal [video], https://doi.org/10.5446/57472, 2022c.

Leung, D. D. V. and dePolo, P. E.: Pyroxene Group, TIB-AV Portal [video], https://doi.org/10.5446/57473, 2022d.

Leung, D. D. V. and dePolo, P. E.: Amphibole Supergroup, TIB-AV Portal [video], https://doi.org/10.5446/57474, 2022e.

Leung, D. D. V. and dePolo, P. E.: Clinojimthompsonite and Chesterite, TIB-AV Portal [video], https://doi.org/10.5446/57475, 2022f.

Leung, D. D. V. and dePolo, P. E.: TotBlocks Palygorskite Group, TIB-AV Portal [video], https://doi.org/10.5446/57476, 2022g.

Leung, D. D. V. and dePolo, P. E.: Sepiolite Group, TIB-AV Portal [video], https://doi.org/10.5446/57477, 2022h.

Leung, D. D. V. and dePolo, P. E.: Kalifersite, TIB-AV Portal [video], https://doi.org/10.5446/57479, 2022i.

Leung, D. D. V. and dePolo, P. E.: Brucite Group, TIB-AV Portal [video], https://doi.org/10.5446/57480, 2022j.

Leung, D. D. V. and dePolo, P. E.: Kaolinite-Serpenting Group, TIB-AV Portal [video], https://doi.org/10.5446/57481, 2022k.

Leung, D. D. V. and dePolo, P. E.: Chlorite Group, TIB-AV Portal [video], https://doi.org/10.5446/57482, 2022l.

Leung, D. D. V. and dePolo, P. E.: How to 3D Print TotBlocks, TIB-AV Portal [video], https://doi.org/10.5446/57483, 2022m.

Thompson, J. B.: An introduction to the mineralogy and petrology of the biopyriboles, Rev. Mineral. Geochem., 9A(1), 141–188, 1981.